Supplementary Information

Green Direct Recycling of Spent $LiFePO_4$ with Reinforced Fe-O d–p Orbital Hybridization for Enhanced Energy Storage Performance

Density functional theory (DFT) simulations

All calculations were performed using density functional theory within the GGA-PBE framework and the projector-augmented wave (PAW) method as implemented in VASP. A plane-wave cutoff of 500 eV and a 3×3×1 k-point mesh was used. A vacuum spacing of 15 Å was applied along the z-direction to avoid spurious slab interactions. Geometry optimization employed energy and force convergence thresholds of 1×10^{-5} eV and 0.02 eV $Å^{-1}$, respectively. vdW interactions were included using the Grimme D3 correction with Becke–Johnson damping (DFT-D3(BJ)), and applied consistently in all structural relaxations, defect calculations, and CI-NEB simulations. Spin-polarized ab-initio molecular dynamics (AIMD) simulations were performed in the NVT ensemble with a Nose–Hoover thermostat at 298 K, using a 0.5 fs time step for 5000 steps. Lithium-ion migration barriers were calculated using the climbing-image nudged elastic band (CI-NEB) method.

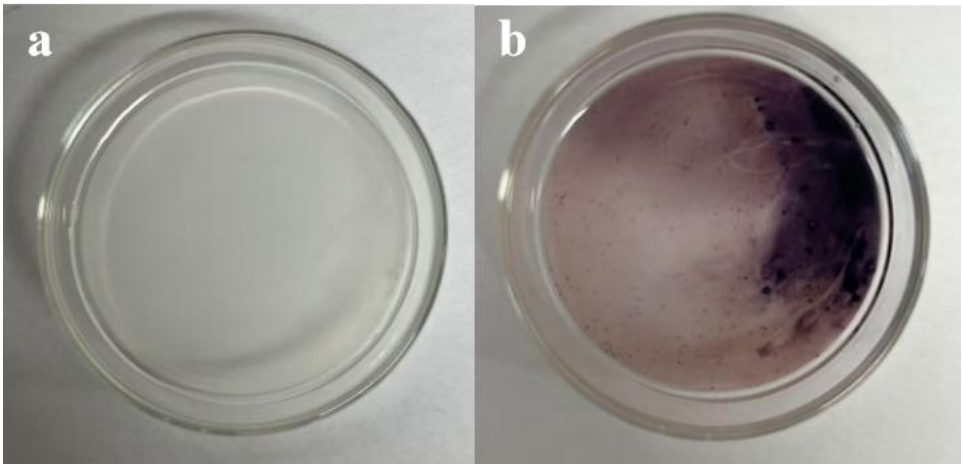

Fig. S1 (a) starch solution; (b) starch solution after color change.

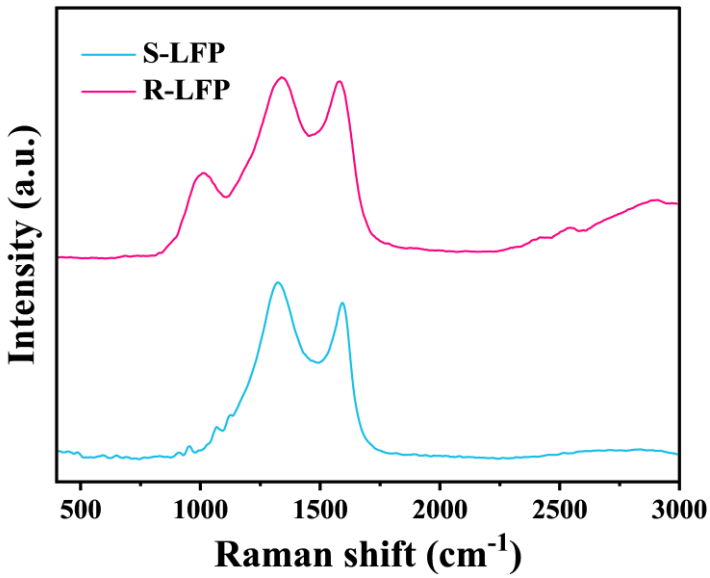

Fig. S2. Raman spectra of S-LFP, R-LFP.

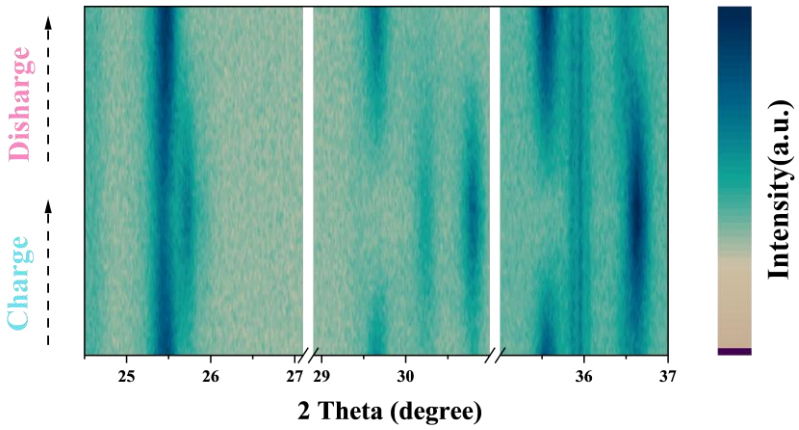

Fig. S3. The initial charge-discharge curve of *in situ* XRD patterns in R-LFP.

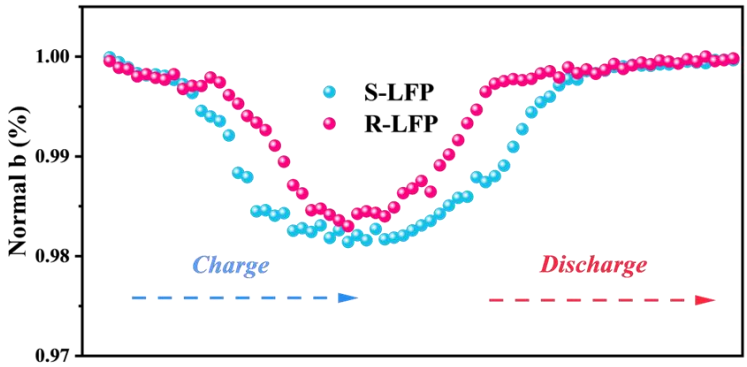

Fig. S4. Normalized b axes variation rates of S-LFP and R-LFP during charge/discharge.

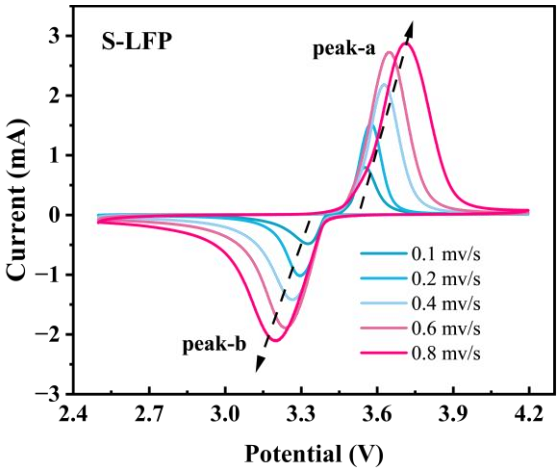

Fig. S5. CV curves at different scanning rates of S-LFP.

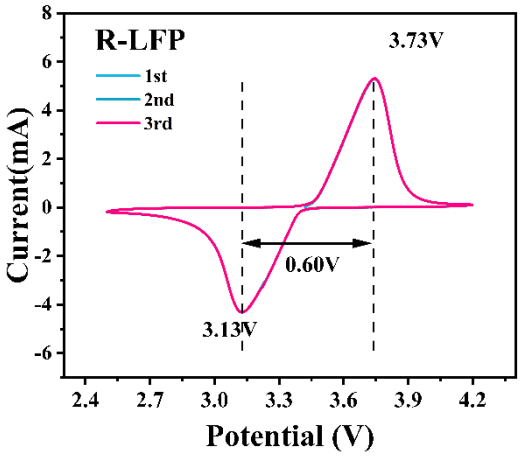

Fig. S6. The initial three CV curves at 1 mV of R-LFP.

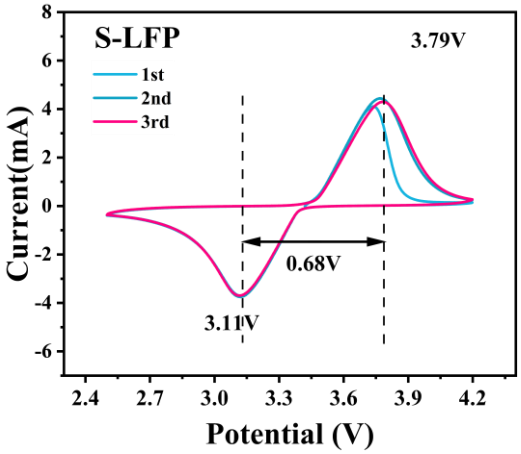

Fig. S7. The initial three CV curves at 1 mV of S-LFP.

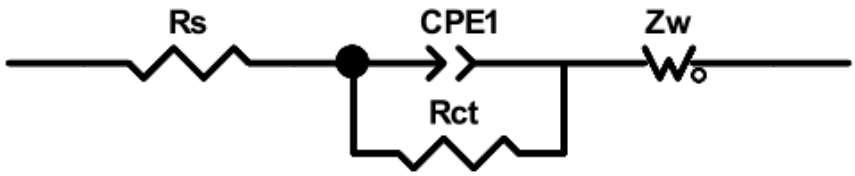

Fig. S8 Equivalent circuit model.

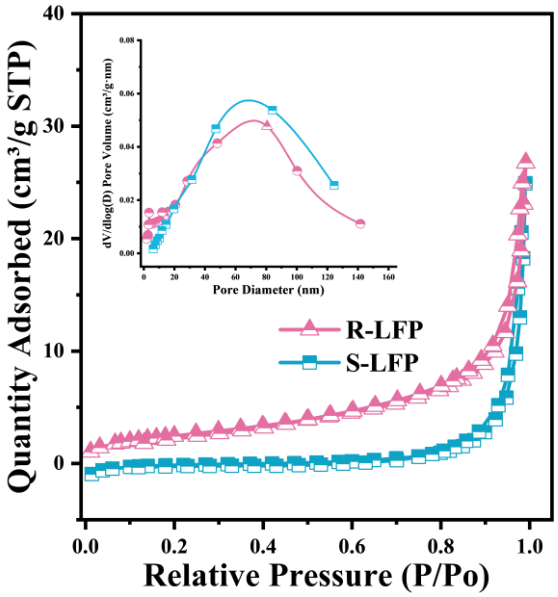

Fig. S9 BET plots of $LiFePO_4$ before and after repair.

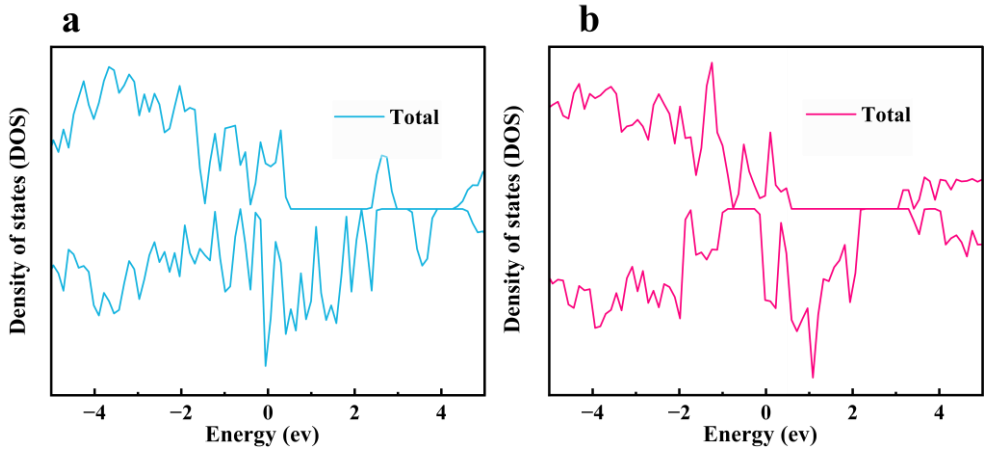

Fig. S10. The Total density of states for (a) S-LFP (b) R-LFP.

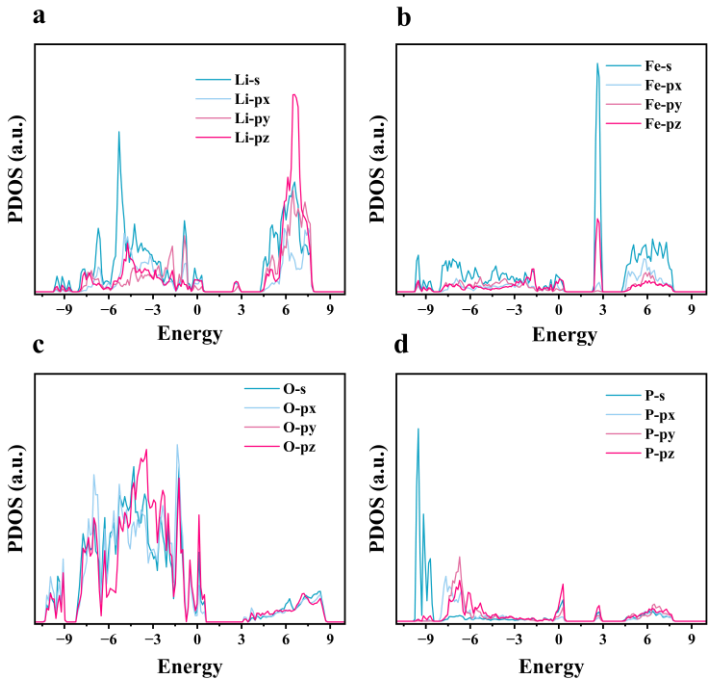

Fig. S11. The partial density of states for S-LFP.

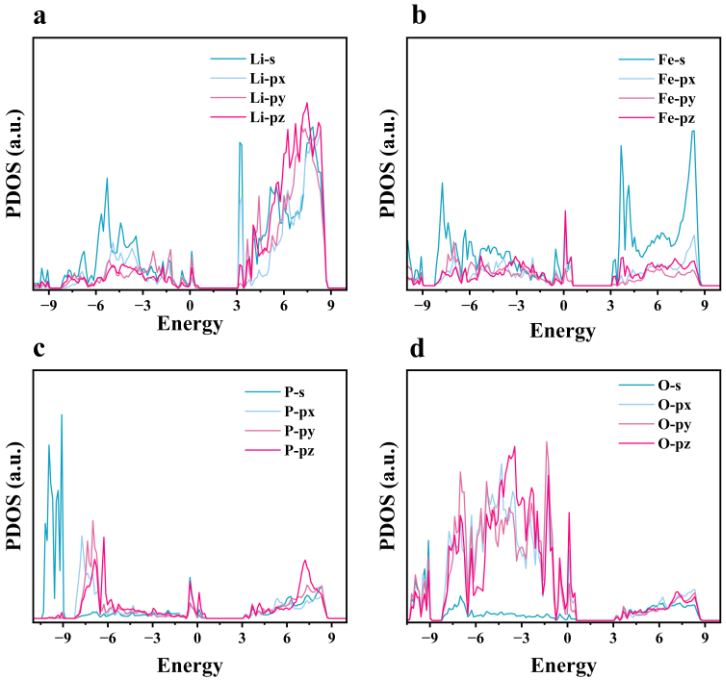

Fig. S12. The partial density of states for R-LFP.

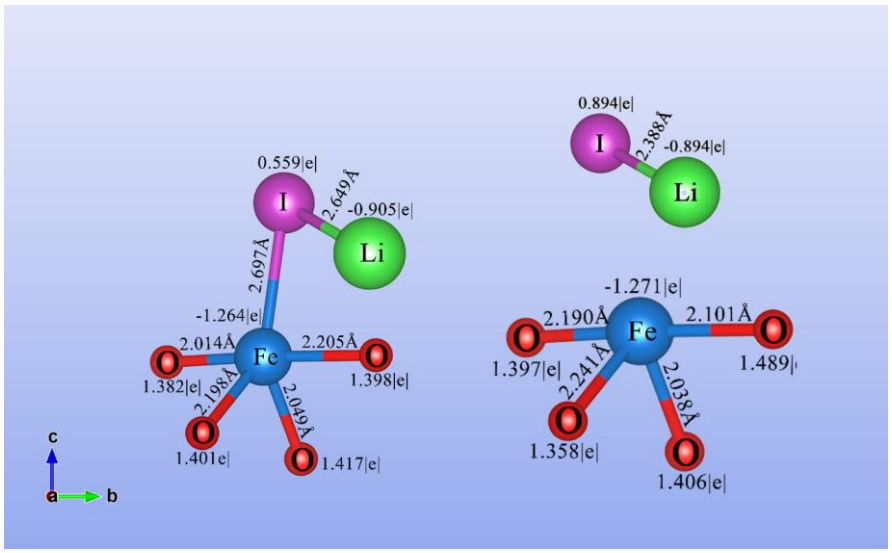

Fig. S13 Selected bond lengths and bader charge of R-LFP, S-LFP and lithium iodide molecule.

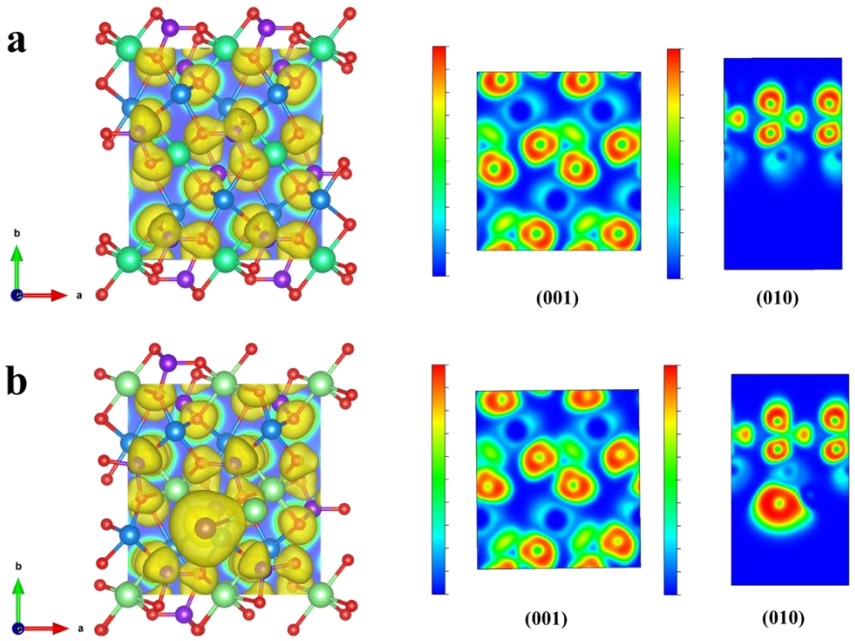

Fig. S14 Electron localization function (ELF) contour plot of the (a) S-LFP and (b) R-LFP. sample.

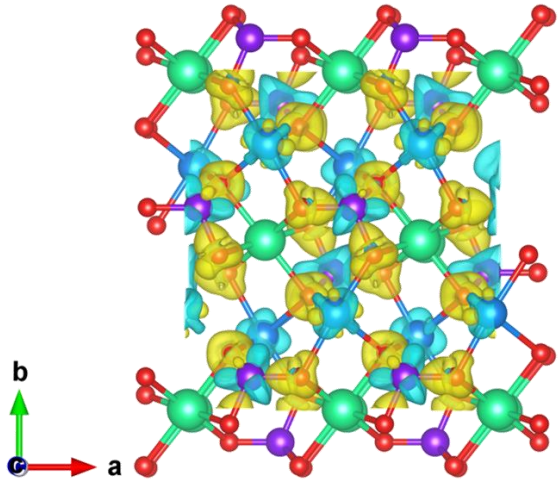

Fig. S15 Charge transfer difference of S-LFP.

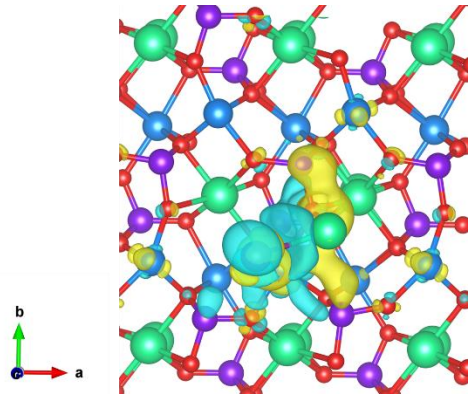

Fig. S16 Top-view differential charge-density map for the R-LFP.

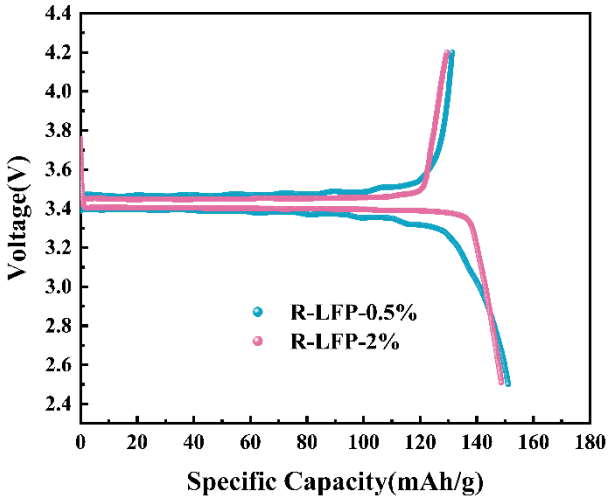

Fig. S17 The initial charge and discharge curves of S-LFP and R-LFP at 0.1 C.

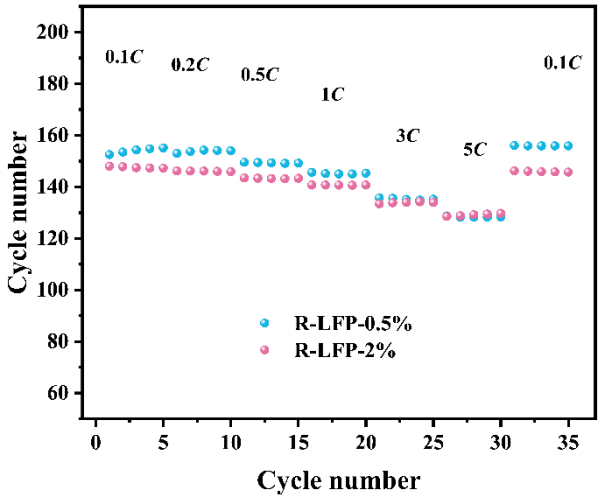

Fig. S18 Rate performance of S-LFP and R-LFP.

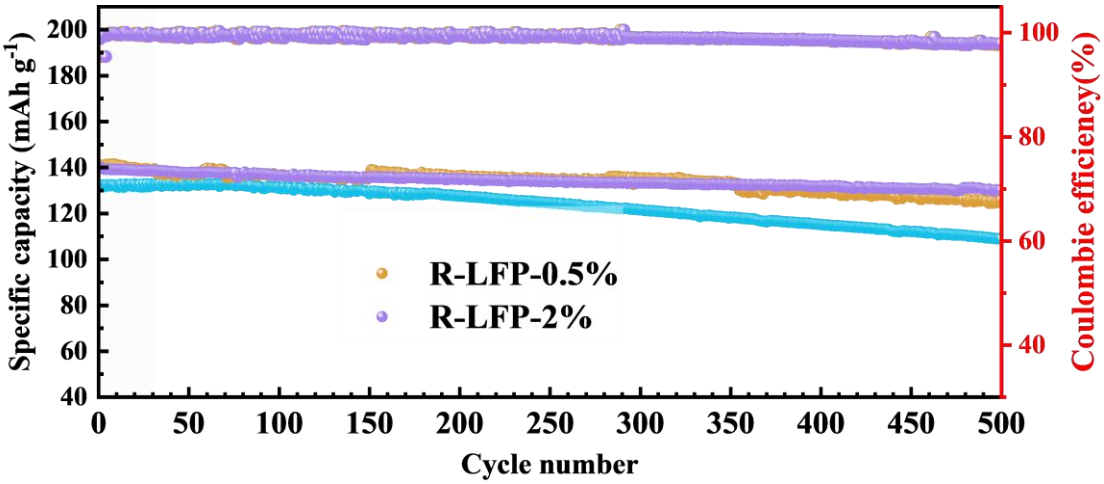

Fig. S19 Cyclic performance of S-LFP, R-LFP at 1 C.

Table S1. Calculated structural parameters from Rietveld refinement of S-LFP, Structural parameters obtained from Rietveld refinement of the X-ray diffraction pattern of S-LFP. Phase 1 $LiFePO_4$: Space group: *Pnma*, a = 10.3298 Å, b = 6.0075 Å, c = 4.6919 Å, V = 291.162 $Å^3$, $\alpha = \beta = \gamma = 90°$， Fraction: 60.40%. Phase 2 $FePO_4$: Space group: *Pnma*, a = 9.8158 Å, b = 5.8838 Å, c = 4.7836 Å, V = 271.846 $Å^3$, $\alpha = \beta = \gamma = 90°$， Fraction:39.60%.

Atoms	x	y	z	OCC	Site
Li1	0	0	0	0.929	4a
Fe2	0	0	0	0.071	4a
Fe1	0.2827	0.2500	0.9743	0.929	4c
Li2	0.2827	0.2500	0.9743	0.071	4c
P1	0.0941	0.2500	0.4180	1.00	4c
O1	0.0966	0.2500	0.7492	1.00	4c
O2	0.4527	0.2500	0.2142	1.00	4c
O3	0.1642	0.0426	0.2798	1.00	8d

Table S2. Calculated structural parameters from Rietveld refinement of R-LFP, Structural parameters obtained from Rietveld refinement of the X-ray diffraction pattern of R-LFP. *Phase*-$LiFePO_4$: Space group: *Pnma*, a = 10. 3264 Å, b = 6.0058 Å, c = 4.6906 Å, V = 290.903 $Å^3$, $\alpha = \beta = \gamma = 90°$, Fraction: 81.38%. Phase 2 $FePO_4$: Space group: *Pnma*, a = 9.8131 Å, b = 5.7873 Å, c = 4.7818 Å, V = 271.564 $Å^3$, $\alpha = \beta = \gamma = 90°$， Fraction:18.62%.

Atoms	x	y	z	OCC	Site
Li1	0	0	0	0.970	4a
Fe2	0	0	0	0.030	4a
Fe1	0.2817	0.2500	0.9744	0.970	4c
Li2	0.2817	0.2500	0.9744	0.030	4c
P1	0.0942	0.2500	0.4186	1.00	4c
O1	0.0970	0.2500	0..7442	1.00	4c
O2	0.4562	0.2500	0.2068	1.00	4c
O3	0.1641	0.0458	0.2830	1.00	8d

Table S3 EIS parameters of LFP before and after repair

Samples	Rs(Ω)	Rct(Ω)	D(cm^2/s)
S-LFP	4.1	243.5	3.35×10^{-13}
R-LFP	1.6	71.1	2.72×10^{-12}

Table S4 BET surface-area and pore-size parameters of $LiFePO_4$.
before and after repair

Thermophysical properties	S-LFP	R-LFP
BET Surface Area (m^2/g)	1.352	9.067
Micropore area (m^2/g)	3.156	10.732
Average pore size(nm)	114.031	18.254

Table S5. Electrochemical performance comparison of recycled LFP cathodes with direct regeneration methods.

No	Methods	Residual capacity (mAh/g)	Restored rate performance (mAh/g)	Cyclic Performance	Ref.
1	Hydrothermal	101 at 0.5C	145 at 0.1C,	97.8% after 100 cycles at 0.5 C	[1]
2	Hydrothermal	139 at 0.1 C, 115 at 1 C	155.1 at 0.1C 114 at 5 C, 87 at 10 C	86 % after 500 cycles at 1 C	[2]
3	Hydrothermal	120 at 0.1 C, 97 at 1 C	162 at 0.2C 120 at 5 C, 102 at 10C	93.7% after 100 cycles at 0.5 C	[3]
4	Hydrothermal	123 at 0.1C, 100 at 1 C	144.4 at 0.1C 115 at 5 C	99% after 100 cycles at 1 C	[4]
5	Hydrothermal	124.3 at 0.1 C, 103 at 1 C	165.9 at 0.1 C, 115.0 at 5 C	95% after 200 cycles at 5C	[5]
6	Solution relithiation	--.	135 at 5C	99% after 100 cycles at 0.5 C	[6]
7	Molten Salt	129 at 0.5 C	145 at 0.1 C 110 at 5 C	95% after 100 cycles at 0.5 C	[7]
8	ultrasound-assisted	153.1 at 0.1C 140 at 1 C	161.6 at 0.1C 154.2 at 1 C 140.3 at 2 C	91% after 200 cycles at 1 C	[8]
9	Solid state sintering	102 at 0.1C 99 at 1 C	146 at 0.1C, 111 at 5 C, 97 at 10C	88% after 400 cycles at 5 C	[9]
10	Solid state sintering	129.8 at 0.2 C 86.6 at 1 C	150 at 0.2 C, 83.2 at 5 C	82% after 300 cycles at 1 C	[10]
11	Solid state sintering	130 at 0.1 C	155 at 0.1C 127 at 5C	87% after 400 cycles at 1 C	[11]
12	Solid state sintering	132.5 at 0.1C	152.3 at 0.1C 112.8 at 5C	94.8% after 100 cycles at 1 C	[12]
13	Chemical relithiation	150 at 0.5C	110 at 5 C, 95 at 10C	85% after 150 cycles at 0.5 C	[13]
14	Electrochemical relithiation	125 at 0.2 C	137.2 at 0.2 C 130 at 2 C. 108 at 5 C	85.5% after 300 cycles at 2 C	[14]
15	Electrically driven process	120.1 at 0.1 C	147.5 at 0.1C 104 at 5 C, 70 at 10 C	95.3% after 500 cycles at 5 C	[15]
16	Electrochemical relithiation	132.46 at 0.1 C	144.9 at 0.1 C 118.7 at 5 C	98% after 100 cycles at 1 C	[16]
17	Hydrothermal	139 at 0.1 C, 115 at 1 C	155.1 at 0.1C 114 at 5 C, 87 at 10 C	84 % after 500 cycles at 1 C	[17]
18	Chemical relithiation	135.6 at 0.1 C	142.4 at 5 C	97.4 % after 500 cycles at 1 C	**This work**

References

[1] J. Song, M. Xiao, T. Chen, F. Wan, X. Guo, *Mater. Lett.* **2024**, *363*, 136333.

[2] D. Tang, G. Ji, J. Wang, Z. Liang, W. Chen, H. Ji, J. Ma, S. Liu, Z. Zhuang, G. Zhou, *Adv. Mater.* **2023**, *36*, 2309722.

[3] P. Xu, Q. Dai, H. Gao, H. Liu, M. Zhang, M. Li, Y. Chen, K. An, Y. S. Meng, P. Liu, Y. Li, J. S. Spangenberger, L. Gaines, J. Lu, Z. Chen, *Joule* **2020**, *4*, 2609.

[4] Y. Yang, Z. Liu, J. Zhang, Y. Chen, C. Wang, *J. Alloys Compd.* **2023**, *947*, 169660.

[5] B. Chen, M. Liu, S. Cao, H. Hu, G. Chen, X. Guo, X. Wang, *J. Alloys Compd.* **2022**, *924*, 166487.

[6] M. Fan, X. Chang, X.-H. Meng, C.-F. Gu, C.-H. Zhang, Q. Meng, L.-J. Wan, Y.-G. Guo, *CCS Chem.* **2023**, *5*, 1189.

[7] X. Liu, M. Wang, L. Deng, Y.-J. Cheng, J. Gao, Y. Xia, *Ind. Eng. Chem. Res.* **2022**, *61*, 3831.

[8] X. Chen, S. Li, Y. Wang, Y. Jiang, X. Tan, W. Han, S. Wang, *Waste Manage. (Oxford)* **2021**, *136*, 67.

[9] G. Ji, J. Wang, Z. Liang, K. Jia, J. Ma, Z. Zhuang, G. Zhou, H.-M. Cheng, *Nat Commun* **2023**, *14*, 584.

[10] T. Wang, C. Gao, Z. Zheng, W. Yu, M. Wang, C. Yang, J. Zhang, *Advanced Functional Materials* **n.d.**, *n/a*, 2502930.

[11] M. Xiao, X. Fu, M. Chen, M. Ye, C. Zhu, F. Wan, X. Guo, *ACS Appl. Mater. Interfaces* **2025**, *17*, 12199.

[12] Y. Wang, Y. Yang, J. Zhang, Y. Chen, C. Wang, *Appl. Surf. Sci.* **2025**, *689*, 162512.

[13] C. Wu, J. Hu, L. Ye, Z. Su, X. Fang, X. Zhu, L. Zhuang, X. Ai, H. Yang, J. Qian, *ACS Sustainable Chem. Eng.* **2021**, *9*, 16384.

[14] *Green Chem.* **2022**, *24*, 6278.

[15] D. Peng, X. Wang, S. Wang, B. Zhang, X. Lu, W. Hu, J. Zou, P. Li, Y. Wen, J. Zhang, *Green Chem.* **2022**, *24*, 4544.

[16] Y. Yang, J. Zhang, H. Zhang, Y. Wang, Y. Chen, C. Wang, *Energy Storage Materials* **2024**, *65*, 103081.

[17] S. Lei, Q. Li, L. Zhang, L. Wang, Y. Yang, *Chem. Eng. J.* **2025**, *511*, 161928.